TAMU TRACER: Targeted Mobile Measurements to Isolate the Impacts of Aerosols and Meteorology on Deep Convection

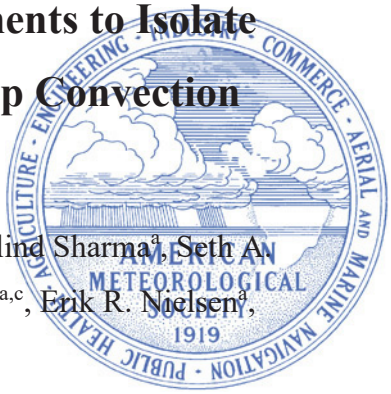

Anita D. Rapp[a*], Sarah D. Brooks[a], Christopher J. Nowotarski[a], Milind Sharma[a], Seth A. Thompson[a], Bo Chen[a], Brianna H. Matthews[a,b], Montana Etten-Bohm[a,c], Erik R. Nielsen[a], and Ron Li[a]

[a] *Department of Atmospheric Sciences, Texas A&M University, College Station, Texas*

[b] *Savannah River National Laboratory, Aiken, SC*

[c] *Department of Atmospheric Sciences, University of North Dakota, Grand Forks, ND*

[*] *Corresponding author*: Anita D. Rapp, arapp@tamu.edu

Early Online Release: This preliminary version has been accepted for publication in *Bulletin of the American Meteorological Society*, may be fully cited, and has been assigned DOI 10.1175/BAMS-D-23-0218.1. The final typeset copyedited article will replace the EOR at the above DOI when it is published.

ABSTRACT

Difficulty in using observations to isolate the impacts of aerosols from meteorology on deep convection often stems from inability to resolve the spatiotemporal variations in the environment serving as the storm's inflow region. During the DOE TRacking Aerosol Convection interactions ExpeRiment (TRACER) in June-September 2022, a Texas A&M University (TAMU) team conducted a mobile field campaign to characterize the meteorological and aerosol variability in airmasses that serve as inflow to convection across the ubiquitous mesoscale boundaries associated with the sea- and bay-breezes in the Houston, Texas, region. These boundaries propagate inland over the fixed DOE Atmospheric Radiation Measurement (ARM) sites. However, convection occurs on either or both the continental or maritime sides or along the boundary. The maritime and continental airmasses serving as convection inflow may be quite distinct, with different meteorological and aerosol characteristics that fixed-site measurements cannot simultaneously sample. Thus, a primary objective of TAMU TRACER was to provide mobile measurements similar to those at the fixed sites, but in the opposite airmass across these moving mesoscale boundaries. TAMU TRACER collected radiosonde, lidar, aerosol, cloud condensation nuclei (CCN), and ice nucleating particle (INP) measurements on 29 enhanced operations days covering a variety of maritime, continental, outflow, and pre-frontal airmasses. This paper summarizes the TAMU TRACER deployment and measurement strategy, instruments, available datasets, and provides sample cases highlighting differences between these mobile measurements and those made at the ARM sites. We also highlight the exceptional TAMU TRACER undergraduate student participation in high impact learning activities through forecasting and field deployment opportunities.

SIGNIFICANCE STATEMENT

The environment influencing storms often varies across scales that are not always adequately captured by measurements collected at fixed locations. This paper describes our strategy for collecting mobile measurements of the aerosols and meteorology that influenced convection initiated by the sea breeze across the Houston, TX region. We show several examples of the local variations in aerosols and meteorology influencing storms that were captured by our mobile platform that were different from those sampled at fixed observation sites. We also highlight potential future studies and science questions that could be addressed using our dataset.

Accepted for publication in *Bulletin of the American Meteorological Society.* DOI 10.1175/BAMS-D-23-0218.1.

CAPSULE (BAMS ONLY)

TAMU mobile measurements capture air mass heterogeneity and meteorology and aerosol environments in convective inflow regions for sea breeze-initiated convection during TRACER field campaign.

Motivation & goals

Deep convective systems play a significant role in a number of critical components of the climate system through their large contribution to the hydrological cycle, feedback on the large-scale circulation, and their radiative effects and importance in regulating climate sensitivity. Aerosol-cloud interactions (ACI) remain one of the most uncertain components in our estimates of total global anthropogenic radiative forcing (IPCC 2021). In deep convection, estimates of the aerosol indirect effect on the top-of-atmosphere radiative forcing through changes in the properties of clouds disagree in magnitude and even sign (e.g., Khairoutdinov and Yang 2013; Fan et al. 2013; Peng et al. 2016; Yan et al. 2014; Koren et al. 2010; Fan et al. 2012). In addition, ACI may alter deep convection precipitation accumulations (Teller & Levin 2006; Wang 2005; Tao et al. 2012), precipitation onset and rate distributions (van den Heever et al. 2011; Lin et al. 2018), updraft intensity and vertical development (Rosenfeld et al. 2008; Fan et al. 2018; Marinescu et al. 2021), and storm electrification (e.g., Williams et al. 2002; Ren et al. 2018; Ren et al. 2019).

Some of the uncertainty in estimates of ACI effects on deep convection stems from the fact that aerosol affects both warm- and cold-phase microphysical processes (Rosenfeld et al. 2008; Sheffield et al. 2015; Fan et al. 2018). However, high-resolution spatiotemporal observations for both the concentrations and physicochemical properties of cloud condensation nuclei (CCN) are often only available from localized field campaigns. There are even fewer observations of ice nucleating particles (INPs) and a still incomplete understanding of ice formation processes (Khain and Pinsky 2018; Kanji et al. 2017) and their role in ACI.

Complicating matters even further, studies have shown that deep convection and the viability of potential ACI effects are modulated by the background meteorological environment conditions, including humidity, wind shear, instability, and storm organization (e.g., Khain 2009; Fan et al. 2009). Moreover, the correlation between CCN and these other

Accepted for publication in *Bulletin of the American Meteorological Society.* DOI 10.1175/BAMS-D-23-0218.1.

environmental factors like CAPE and the level of neutral buoyancy make it especially difficult to separate the ACI radiative response from the meteorology (Varble et al. 2018).

On top of the meteorological considerations, many previous studies of ACI do not realistically account for the full horizontal and vertical variations of aerosols in the storm environment (Lebo 2014), especially in regions where significant mesoscale boundaries exist, such as the sea breeze in the Houston, TX region. *The continued conflicting results of ACI in deep convection in both observational and modeling studies highlights the need for careful analysis and better observations to advance our understanding of ACI and isolate their effects from other meteorological environmental effects.*

To address this, the Department of Energy (DOE)-funded TRacking Aerosol Convection interactions expERiment (TRACER; Jensen et al. 2019) focused on collecting high spatial and temporal resolution observations of the properties of convection, as well as the thermodynamic and aerosol environment in which the convection occurs. The Houston, TX region was chosen for TRACER because of its diversity of aerosol conditions and consistent isolated convection initiated by the sea breeze (Fridland et al. 2019), as well as its long history as the basis for air quality studies (e.g., Daum et al. 2004; Parrish et al. 2009; Atkinson et al. 2010; Wright et al. 2010) and both observational and model studies on ACI (e.g., Orville et al. 2001; Jin et al. 2005; Fan et al. 2008; Carrio et al. 2010; Hu et al. 2019; Fan et al. 2020; Zhang et al. 2021 among many others). A full suite of atmospheric state, cloud, aerosol, and precipitation measurements were collected from October 2021-September 2022 at two fixed site locations, the first Atmospheric Radiation Measurement (ARM) Mobile Facility (AMF1) located at LaPorte, TX near the Galveston Bay and an ancillary site (ANC) that collected measurements from June – September 2022 in a more rural area outside of the Houston metropolitan area, with the second generation C-band Scanning ARM Precipitation Radar (CSAPR2) in between for radar coverage of both sites. An Intensive Operation Period (IOP) occurred from June-September 2022 where the CSAPR2 operated in an automated cell tracking mode (Lamer et al. 2023) and radiosondes were launched with increased frequency on days designated by the forecast and science team for enhanced operations. Days with a strong sea breeze in an environment conducive to isolated convection were considered ideal conditions for enhanced operations.

Summertime deep convection in the Houston region typically occurs in onshore flow regimes west of the semi-permanent Bermuda High with relatively large instability and

Accepted for publication in *Bulletin of the American Meteorological Society.* DOI 10.1175/BAMS-D-23-0218.1.

limited vertical wind shear. Foci for convection initiation are provided by both the inland-propagating sea-breeze front from the Gulf of Mexico (GOM) and/or the westward propagating bay-breeze front associated with Galveston Bay (Fig. 1). Once initial convection has developed, outflow often reinforces both the sea- and bay-breeze fronts or produces new outflow boundaries capable of triggering subsequent convection. Typically, there are several mesoscale air masses in the Houston region on a convective day: maritime GOM air south of the sea-breeze front, maritime Galveston Bay air southeast of the bay-breeze front, continental air north of the sea- and bay-breeze fronts, and air disturbed by recent convective outflow. Each air mass is likely to have significantly different thermodynamic and aerosol vertical profiles which may be ingested by proximate convection such that horizontal adaptability in measurements is critical to have any hope of disentangling aerosol effects from meteorology.

Full understanding of ACI requires co-located meteorological and aerosol profiling at multiple sites spread across different air masses where convection is initiated. The overarching goal of the Texas A&M University (TAMU) TRACER field campaign was to *provide meteorological and aerosol profiles of air masses unsampled by the fixed ARM sites in the context of the convection initiated by the inland propagating sea breeze.* To achieve this goal, we deployed a suite of mobile measurements in conjunction with DOE ARM TRACER facilities from June - September 2022 to measure the thermodynamic, kinematic, and aerosol populations in different air masses across the sea- and bay-breeze fronts on days of sea-breeze initiated convection. This combination of fully mobile aerosol measurements and thermodynamic and kinematic observations provides a unique set of observations that captures the near-storm environments to better represent the inflow air mass that is actually influencing deep convection. This paper provides an overview of the TAMU TRACER deployment strategy, measurements, preliminary case studies, and some planned analysis and possible science opportunities for ACI-related studies and beyond.

Accepted for publication in *Bulletin of the American Meteorological Society.* DOI 10.1175/BAMS-D-23-0218.1.

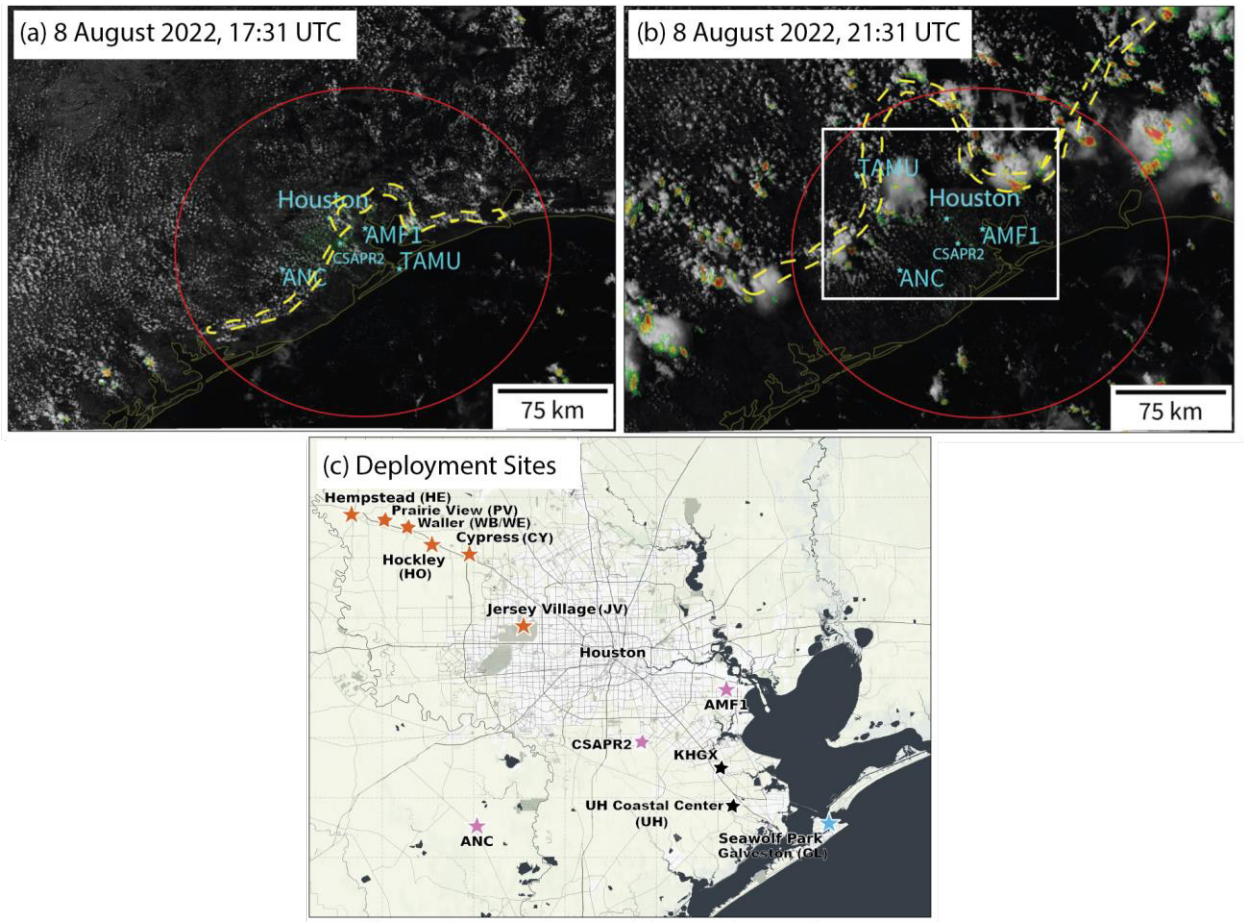

Figure 1. GOES-16 visible satellite image overlaid with KHGX WSR-88D reflectivity in the Houston region showing the estimated position of the sea-and bay-breeze front (dotted-dashed line), DOE ARM AMF1, ANC, and CSAPR2 sites and the TAMU deployment locations (blue stars) typical of our (a) early afternoon deployment in a maritime air mass, and (b) late afternoon deployment in a continental air mass. Red line indicates 150-km range ring from KHGX. (c) Map of region inside white box in (b) showing TAMU maritime (light blue star) and continental (red stars) deployment sites indicated in Table 2 as well as DOE AMF1, ANC, CSAPR2 (purple stars), and KHGX and UH coastal center deployment locations (dark blue stars).

TAMU TRACER field campaign

Instrumentation and measurements

Throughout the TAMU TRACER field campaign, iMet-4/4c radiosondes were used to obtain profiles of pressure, temperature, relative humidity (RH), wind speed, and wind direction at a temporal resolution of one second. For more information about sensor details, iMet software, and uncertainties, interested readers can visit https://www.intermetsystems.com/products/imet-4-radiosonde/.

For the duration of each deployment, conventional meteorological surface observations (pressure, temperature, humidity, wind speed, and direction) were collected using a portable

Accepted for publication in *Bulletin of the American Meteorological Society*. DOI 10.1175/BAMS-D-23-0218.1.

Met One AIO 2 Sonic Weather Sensor (SWS; https://metone.com/products/aio-2-sonic-weather-sensor/). The self-contained sensor was deployed on a 2-m tripod over an open grassy surface at each site with an internal compass for automatic direction finding. Three-minute averages of each variable were archived.

TRACER marked the first deployment of the Texas A&M Rapid Onsite Atmospheric Measurement Van (ROAM-V), a fully mobile and customizable laboratory. Five rechargeable lithium-ion batteries (Big Battery Rhino 276AH LiFePO4) allow for continuous and untethered sampling with ROAM-V for up to eight hours without the risk of self-contamination from engine or generator exhaust. Additionally, an isokinetic inlet enables in-transit sampling at reduced speeds if needed. During TRACER, ROAM-V was outfitted with a suite of aerosol instruments that focused on measuring cloud-forming properties (Table 1). In-situ measurements included aerosol concentration (unsized and sized) and CCN concentration. While a Condensation Particle Counter (CPC) sampled unsized concentrations, sized concentrations were measured by a Scanning Mobility Particle Sizer (SMPS) and a Portable Optical Particle Spectrometer (POPS) with a combined size range of 7.23-3370 nm. For CCN concentrations, a CCN Counter scanned through 6 supersaturations (0.2, 0.4, 0.6, 0.8, 1.0, and 1.2%) at 5-minute intervals. Ambient aerosol was also collected through impaction for offline ice nucleation and single particle analyses. The Davis Rotating Uniform size-cut Monitor (DRUM) was used for impaction and has a series of 4 impactors (>3, 3-1.2, 1.2-0.34, and 0.34-0.15 μm). To minimize contamination, aerosol was collected onto pre-combusted aluminum foil substrates and, after each deployment, stored at -80°C until ice nucleation analysis at Texas A&M (Alsante et al. 2023). In addition to the INP concentration measurements provided by the DRUM deployed on the ROAM-V, INP concentrations were measured at AMF1 and the ANC through deployment of two additional DRUM samplers and offline analysis in the Brooks laboratory at Texas A&M University campus. Instrumentation comparable to the other ROAM-V instrumentation was operated by the DOE at AMF1.

Accepted for publication in *Bulletin of the American Meteorological Society.* DOI 10.1175/BAMS-D-23-0218.1.

Figure 2. (left) ROAM-V and (right) instrument payload during TRACER.

Table 1. Instrument payload during TAMU TRACER.

Instrument	**Model**	**Variables**
iMet-4 radiosonde	InterMet 4/4c	Pressure, Temperature, Relative Humidity, Wind Speed, Wind Direction
Sonic Weather Sensor (SWS)	Met One AIO 2	Pressure, Temperature, Relative Humidity, Wind Speed, Wind Direction
Condensation Particle Counter (CPC)	GRIMM CPC 5.403	Aerosol concentration; 4.5-625 nm
Scanning Mobility Particle Sizer (SMPS)	TSI 3750, 3082, 3088, 3081A	Aerosol size distribution; 7.23-305.1 nm
CCN Counter	DMT CCN-100	CCN concentration; 0.2, 0.4, 0.6, 0.8, 1.0, and 1.2% supersaturation
Davis Rotating Uniform size-cut Monitor (DRUM)	DRUMAir DA400	Aerosol impactor for offline ice nucleation and composition analyses; >3, 3-1.2, 1.2-0.34, and 0.34-0.15 µm size-cuts

Accepted for publication in *Bulletin of the American Meteorological Society.* DOI 10.1175/BAMS-D-23-0218.1.

Portable Optical Particle Spectrometer (POPS)	Handix POPS	Aerosol size distribution; 125-3370 nm
Continuous Flow Diffusion Chamber (CFDC)	Handix CFDC-IAS	Online ice nucleation
Mini Micro Pulse Lidar (MPL) Combined MPL, SMPS, POPS, CCN and DRUM INP	DMT MiniMPL	Vertical profile; 532 nm laser, backscatter and depolarization Aerosol vertical profiles CCN vertical profiles INP vertical profiles

The ROAM-V instrument suite also included a 532 nm mini Micro Pulse Lidar (miniMPL) to measure the vertical profile of backscatter and depolarization by aerosols and cloud particles. Using the ROAM-V aerosol, CCN, and INP and the radiosonde data as inputs, the MPL observations can be used to produce vertical profiles of aerosol, CCN and INP concentration (Ghan and Collins 2004; Ghan et al. 2006; Marinou et al. 2019; Lenhardt et al. 2023). First, operating on the assumption that the measured aerosol population and its cloud forming properties are representative of those aerosols aloft, we can use the ROAM-V aerosol concentration and size distribution measurements are used to convert lidar backscatter into an aerosol concentration profile. Next the ROAM-V CCN measurements are used to prescribe the subsaturated hygroscopicity and subsequent growth of the aerosol population at ambient relative humidities provided by the radiosonde data to generate a humidity-corrected aerosol profile. In addition, the ROAM-V CCN measurements are used to estimate the concentration of aerosols which would activate at supersaturations of 0.2 to 1.2%. The ROAM-V ice nucleation measurements provide the fraction of the aerosol population that can act as ice nucleating particles as a function of temperature. These data are combined with the aerosol profiles to produce vertical profiles of INP.

Primary deployment strategy

The guiding mission for our mobile deployment strategy was to sample vertical profiles of meteorological variables and aerosol concentrations simultaneously with the ARM fixed-site measurements, but within a different air mass (typically defined by the position of the sea-breeze front). For a typical observing day, this involved two separate ~3-hour deployments.

Accepted for publication in *Bulletin of the American Meteorological Society.* DOI 10.1175/BAMS-D-23-0218.1.

The first deployment was generally in late morning through early afternoon on the GOM coast in Galveston, TX to sample the air mass on the maritime side of the developing sea-breeze front (hereafter "maritime air mass"). At this time, the AMF1 and ANC sites were typically on the inland side of the sea breeze front (hereafter "continental air mass") or often the AMF1 site was in a maritime air mass representative of Galveston Bay, but not necessarily the GOM (Fig. 1a).

Later in the day, generally mid-to-late afternoon, the sea-breeze front and/or bay-breeze front, often augmented by convective outflow boundaries, would push inland beyond the AMF1 and ANC sites, placing them both in a maritime or convective outflow air mass. To fulfill our mission, the TAMU team would redeploy at a site on the inland side of the new boundary position, to sample a continental air mass (Fig. 1b). Our late afternoon inland site selection varied depending on the inland propagation speed of the sea-breeze front/outflow boundaries and locations of active convection (see Fig. 1c), with the goal of sampling the undisturbed late-day continental air mass for 2-3 hours.

Secondary deployment strategies

In practice, conditions occasionally necessitated a shift to secondary mission goals. These included longer (~6 hours) single-site continental air mass heterogeneity measurements at an inland site NW of Houston if early morning convection disturbed the maritime air mass or if another team was collecting measurements near the coast. For prolonged, single-site continental deployments, a site was typically chosen such that it would be within a different air mass from the AMF1 or ANC site for most of the deployment, or that we would sample both the inflow and outflow of nearby convection during the deployment. Another secondary mission goal for the late afternoon deployment was targeting air mass recovery after a boundary passage in cases where convection ahead of the sea breeze front was more widespread than expected and no undisturbed air mass was within range of the CSAPR2.

TAMU TRACER also included radiosonde-only and aerosol-only missions. The radiosonde-only missions generally targeted the primary and secondary goals listed above (Table 2). ROAM-V deployed without the radiosonde team to the University of Houston Coastal Center for long-term collection of background aerosol conditions and to the AMF1 site for instrument calibration and comparison missions (Table 3).

Accepted for publication in *Bulletin of the American Meteorological Society.* DOI 10.1175/BAMS-D-23-0218.1.

Deployment procedure

A typical deployment of the mobile radiosonde team and ROAM-V generally proceeded as follows: the mobile radiosonde team deployed two radiosonde ground stations (an iMet 3050a and an iMet 3150 system) for redundancy and the SWS for conventional meteorological surface observations for the deployment duration. The ROAM-V would park upwind to sample air undisturbed by exhaust from other nearby vehicles.

The mobile radiosonde team timed launch to coincide with one of the ARM enhanced IOP radiosonde launch times (1800, 1930, 2100, or 2230 UTC). In practice, this timing was typically achieved at the Galveston maritime site, but radiosondes at the inland (usually continental) sites were often launched ad hoc (but within an hour of ARM launches) to avoid active convection or boundary passage (e.g., Figure 5). Radiosonde launches were generally terminated at 100-hPa (after about 1 hour), at which point data were archived and sounding diagrams were shared in real-time with other TRACER teams. During the radiosonde setup,

Table 2. List of deployment dates and measurements categorized by sampled airmass, the time of the radiosonde launch(es) (R), the location of each airmass in parentheses after the radiosonde launch time, and the collection period of CPC aerosol and lidar sampling (A), for each air mass. All times given in UTC. Shaded rows represent dates following the primary deployment strategy of early afternoon maritime airmass sampling and late afternoon continental airmass sampling. On days of secondary strategy, the notes column indicates the reasoning.

Date	Maritime	Continental	Outflow/Other	Notes
2 Jun		R: 2030 (WB)	R: 2330 (WB)	NSF ESCAPE team sampled coastal environment; Sampled post-frontal continental airmass at 2330
21 Jun		R: 1900, 2200 (WB)		ESCAPE team sampled coastal environment; launch at 1900 sampled continental air mass modified by outflow
22 Jun		R: 2041 (WB)		ESCAPE team sampled coastal environment; later launches scrubbed due to increased storm coverage
26 Jun	R: 1858	R: 2324 (WB)		
29 Jun		R: 1726, 2033 (WB)		ESCAPE team sampled coastal environment; offshore tropical disturbance hindered sea breeze development
6 Jul		R: 1900, 2150 (WB)		ROAM-V unavailable
11 Jul	R: 1900	R: 2327 (WB)		
12 Jul			R: 2139, 2329 (WE) A: 2123-0105	Changed mission strategy to sample the near-storm inflow and outflow air masses

Accepted for publication in *Bulletin of the American Meteorological Society.* DOI 10.1175/BAMS-D-23-0218.1.

13 Jul	R: 1730 A: 1644-1853	R: 2204 (WE) A: 2118-2321		
27 Jul	R: 1732 A: 1611-1829	R: 2124 (WB)		
28 Jul	R: 1727		R: 2132 (WE) A: 2045-2310	Changed mission strategy to sample outflow airmass during second deployment
29 Jul	R: 1724 A: 1708-1834		R: 2108 (WE) A: 2102-2233	Convectively modified continental airmass sampled at the second deployment
30 Jul	R: 1731 A: 1626-1838	R: 2105 (CY) A: 2100-2238		
7 Aug	R: 1722	R: 2127 (HE)		
8 Aug	R: 1724 A: 1629-1847	R: 2131 (HE) A: 2122-2252		
9 Aug	R: 1726 A: 1633-1902	R: 2139 (HE) A: 2137-2310		
10 Aug		R: 1720, 2031 (JV) A: 1715-2145	R: 2242 (JV) A: 2242-2333	Multicellular convection near the coast; mission strategy changed to sample continental airmass; convective outflow reached launch site at 2242
21 Aug		R: 1728, 1858 (WE) A: 1707-2104		Sea breeze washed out by convection along the coast; ARM sites in different airmass
22 Aug			R: 1738 (HO) A: 1726-2012	Sea breeze did not develop, but cloud fields indicated heterogeneous air masses between TAMU and ARM
26 Aug	R: 1726 A: 1614-1842	R: 2134 (PV) A: 2138-2250		
27 Aug		R: 1724 (HE) A: 1638-1748, 2039-2135	R: 1905, 2039 (HE) A: 1748-2019	Inland-only due to early morning coastal convection; outflow boundary from nearby convection passed prior to 2nd launch
28 Aug	R: 1728 A: 1637-1850	R: 2119 (HO) A: 2126-2301		
31 Aug	R: 1729 A: 1639-1850			Scrubbed 2nd mission due to numerous convective cells rapidly developing over inland site
6 Sep		R: 1730, 1904 (HO) A: 1655-2053		Inland-only due to cloud cover and morning showers near the coast
7 Sep		R: 1700, 1900, 2030 (HO) A: 1640-2148		No ARM enhanced operations; sampled pre-convective inland environment for convection along a frontal boundary
17 Sep	R: 1718 A: 1649-1825	R: 2059 (HO) A: 2115-2221		
18 Sep	R: 1726 A: 1653-1831	R: 2126 (HO) A: 2116-2219		
19 Sep	R: 1659 A: 1633-1824	R: 2059 (HE) A: 2056-2217		
25 Sep	R: 1729 A: 1618-1850	R: 2200 (HO) A: 2113-2300		

Accepted for publication in *Bulletin of the American Meteorological Society.* DOI 10.1175/BAMS-D-23-0218.1.

Table 3. ROAM-V aerosol-only deployment date, site, and collection period.

Date	Site	Collection period (UTC)
20 Jul	GL	1700-2035
22 Jul	GL	1914-2009
26 Jul	UH	1753-2238
18 Aug	AMF1	1706-2157
23 Aug	UH	1507-2228
24 Aug	UH	1447-1836
1 Sep	AMF1	1734-2224
9 Sep	AMF1	1559-2004
21 Sep	UH	1353-2107
22 Sep	UH	1339-2110
23 Sep	UH	1338-2056

launch, and ascent, the ROAM-V continuously collected surface aerosol and lidar profiling measurements to provide requisite data for collocated, simultaneous CCN and INP profiles within the air mass. Once the radiosonde data collection was complete and the ROAM-V had collected at least two full hours of aerosol observations, the team would transit to the second deployment location or return to TAMU. During longer single-site deployments, multiple radiosondes were launched with continuous surface meteorology and aerosol sampling for the entire deployment.

Deployment decisions and site selection

The decision of when and where to deploy was made jointly by the rotating pair of forecasting and deployment leaders (faculty members or research staff) with the goal of targeting days where a clearly defined sea-breeze front was expected to initiate relatively isolated convection. If ARM declared the next day as an enhanced sounding day for their facilities, the TAMU deployment and forecast teams would meet to determine if the scenario met our primary or secondary deployment goals. If so, the meeting transitioned to logistics and operations to plan the next day's schedule and preliminary site selections.

Candidate deployment sites were selected in advance to identify locations that were publicly accessible, had a large open parking lot with relatively little traffic, and did not have obvious point sources of aerosols immediately upwind. Most deployment sites were at public parks or schools. Throughout the project we deployed to one maritime site and seven different continental sites (Figure 1c, Table 2) because afternoon convective evolution differed considerably from day to day. In conjunction with the nowcasting support team on TAMU's campus, a continental site was often determined during the mobile team's inland

Accepted for publication in *Bulletin of the American Meteorological Society.* DOI 10.1175/BAMS-D-23-0218.1.

transit. For primary missions, we targeted a location within range of the CSAPR2 radar but far enough removed from active convection, outflow boundaries, and the sea breeze front so that radiosonde(s) could be launched in an unmodified continental air mass.

Student High Impact Learning Experience (or colored inset box)

TAMU TRACER represented a tremendous high-impact learning experience for students, and would not have been possible without their involvement. In total 16 graduate students and 19 undergraduate students, many from underrepresented groups in science, participated in TAMU TRACER through field deployments, forecasting/nowcasting, and operational support (Figure 3). Each field deployment involved a rotating crew of 1-2 faculty/research staff, 2-3 graduate students, and 2-3 undergraduate students. In the field, students were responsible for deploying and maintaining the aerosol equipment and SWS, as well as launching radiosondes under the guidance of the faculty/research staff deployment leader. Observing days typically began around 7:30 AM local time with return as late as 9:30 PM to the TAMU campus in College Station, TX (~90 miles northwest of Houston), often requiring exhausting 12 to 15-hour days in over 100°F heat and humid conditions.

Students were also assigned rotations as the daily forecaster/nowcaster and on-campus deployment support staff. Under the guidance of the forecast leader, the daily student forecaster prepared customized short-term and extended-range forecasts of sea-breeze front location and convection likelihood, with recommendations for potential future deployment days. Another student provided remote nowcasting support for the deployment team, providing updates on sea-breeze front location and active convection/outflow, and making calls to local airports/Federal Aviation Administration (FAA) centers for balloon launch clearance. Many of our students also participated in preparing briefing slides or gave parts of forecast briefings for the TRACER-wide daily forecast discussion.

Student participation was solicited and supported through a unique mix of paid positions, research credits, and volunteerism. Prior to the campaign, we offered a 1-credit directed studies course in Spring 2022, where prospective undergraduate student participants were trained on the aerosol and radiosonde equipment, aerosol-cloud interactions, sea breeze and convection forecasting, and our operating procedures. DOE ASR funds partially supported 3 graduate students and 6 hourly part-time undergraduate students. Undergraduate employment and travel were also subsidized through TAMU College of Arts & Sciences (formerly

Accepted for publication in *Bulletin of the American Meteorological Society.* DOI 10.1175/BAMS-D-23-0218.1.

Geosciences) High Impact Learning Experience funds. Other undergraduates were incentivized to participate through a points-based system, where different TRACER-related activities described above accrued points towards undergraduate research credits, resulting in 1-4 research credits per student. Alternatively, many graduate students and some undergraduates participated entirely on a volunteer basis for experience.

Figure 3. TAMU ROAM-V and mobile radiosonde teams on a deployment, graduate students operating instruments in ROAM-V, undergraduates launching radiosondes, and a subset of the faculty, research staff, and graduate and undergraduate student participants in TAMU TRACER.

Example deployment and data

The section below highlights an example of the TAMU TRACER dataset compared to AMF1 measurements for one of our primary missions targeting maritime and continental air mass heterogeneity across the sea-breeze front. On the morning of 8 August 2022, the synoptic environment was conducive to the development of a sea breeze in southeast Texas.

Accepted for publication in *Bulletin of the American Meteorological Society.* DOI 10.1175/BAMS-D-23-0218.1.

A ridge pattern at the 500 hPa level led to mid-tropospheric convergence, resulting in high surface pressure over the southern CONUS. The southeasterly onshore flow associated with this high-pressure system facilitated the advection of low-level moisture from the GOM over the TRACER domain, providing sufficient instability for deep convection initiation. The presence of weak synoptic-scale onshore winds, combined with the absence of short-wave disturbances (i.e., weak large-scale ascent), created ideal conditions for the development of a sea-breeze circulation. As the land-sea temperature gradient gradually strengthened throughout the afternoon, the sea breeze propagated inland.

The first TAMU radiosonde launch at 1724 UTC sampled the maritime air mass, as the sea-breeze front had already propagated ~50 km inland from the coast (Fig. 1a). Based on the visible satellite imagery in Figure 1a, the AMF1 radiosonde likely sampled a mixture of GOM and Galveston Bay maritime air mass, while the sea breeze was still south of ANC where the continental air mass was sampled. The simultaneous sampling of the background environment from the three different sites revealed fine-scale spatial heterogeneity in the mesoscale environments of deep convection. In the first sounding (Fig. 4a), even though the TAMU and AMF1 sites were under the influence of a maritime air mass, the mixed-layer CAPE (MLCAPE) at AMF1 was much larger (2130 J kg^{-1}) compared to the TAMU site (1781 J kg^{-1}). This difference in instability can be primarily attributed to relatively large values of near-surface dewpoint temperature and a steeper lapse rate within the 850-500 hPa layer at the AMF1 site. These values were very typical of early afternoon deployments, falling close to the median MLCAPE values of 1780 J kg^{-1}at the TAMU site and 2118 J kg^{-1}at the AMF1 for the entire TAMU TRACER campaign. The ANC site (not shown) had a much deeper well-mixed layer (surface to 800 hPa), with little potential instability above the 700 hPa level, resulting in the least MLCAPE (1346 J kg^{-1}), which was lower than the typical TAMU TRACER campaign median MLCAPE value (1817 J kg^{-1}) for the ANC in the early afternoon.

The timeseries of ROAM-V aerosol concentrations (Fig. 4b) shows relatively large background aerosol concentrations for a maritime air mass, near 2000 cm^{-3} with intermittent spikes, which we attribute to ship exhaust from the nearby Houston ship channel. Surprisingly, the relatively “clean” maritime background air mass had unexpectedly large aerosol concentrations throughout the TRACER campaign. The fine-scale heterogeneity

Accepted for publication in *Bulletin of the American Meteorological Society.* DOI 10.1175/BAMS-D-23-0218.1.

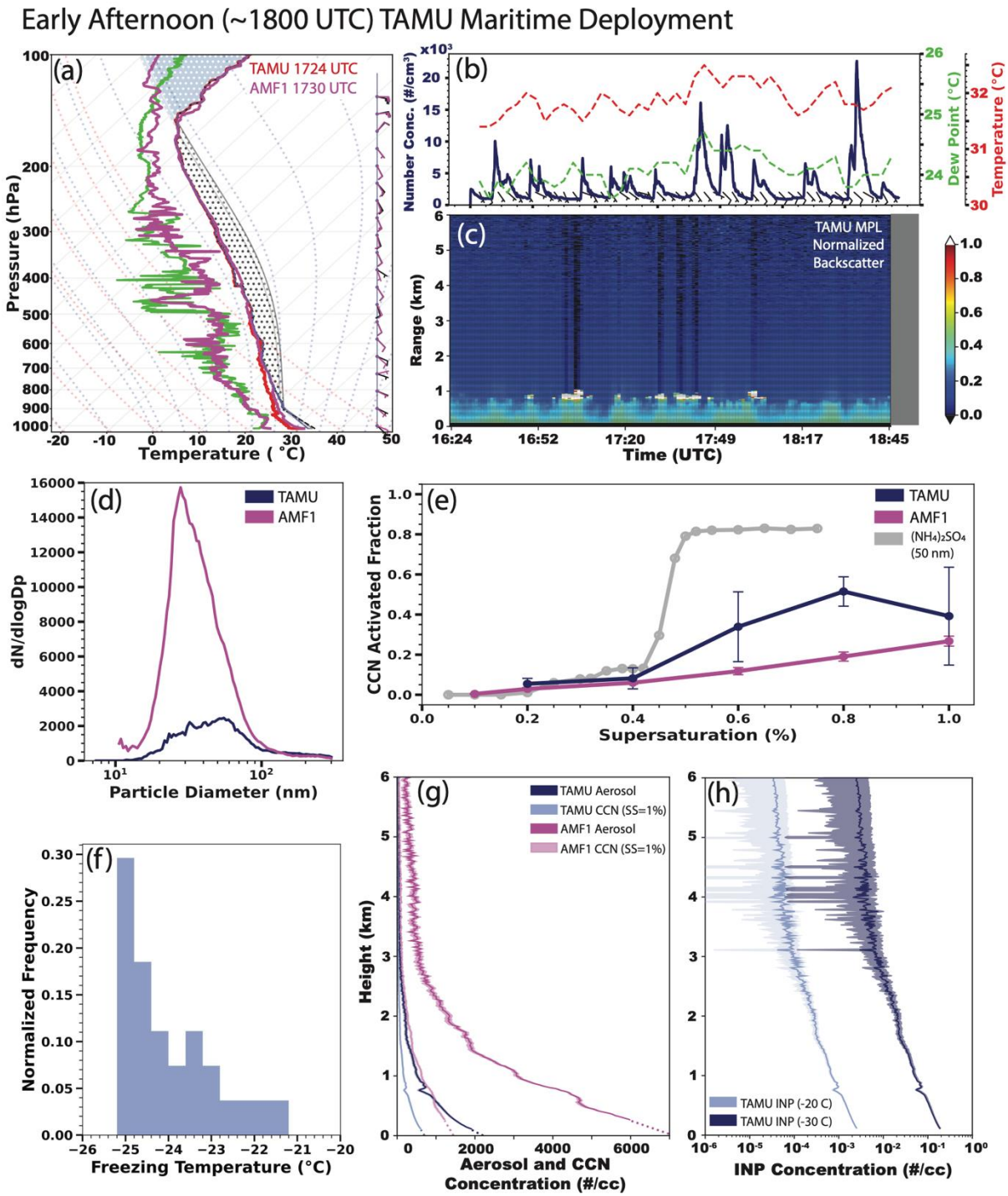

Figure 4 - a) 1800 UTC TAMU and AMF1 SkewT-logP comparison, b) CPC aerosol concentration and SWS temperature, dewpoint, and winds, c) miniMPL backscatter, d) TAMU and AMF1 SMPS aerosol size distributions, e) TAMU and AMF1 CCN activated fraction, f) INP freezing temperatures, g) TAMU and AMF1 retrieved profile of aerosol and CCN concentration, and h) retrieved TAMU INP concentration profile for early afternoon maritime deployment at Seawolf Park in Galveston, TX on 8 August 2022. Shading on panels g) and h) represent the uncertainty range due to lidar inversion process and hygroscopic growth corrections. TAMU maritime is represented in blue with AMF1 maritime represented in magenta.

observed in the mesoscale thermodynamic environment shows an even greater contrast in aerosols. The bay breeze maritime air mass at the AMF1 site, with nearby industry and

Accepted for publication in *Bulletin of the American Meteorological Society.* DOI 10.1175/BAMS-D-23-0218.1.

refineries, showed notably larger aerosol concentrations shifted toward smaller sizes than those sampled in the sea breeze maritime air mass (Fig. 4d). Both sites showed relatively small observed CCN activated fractions at greater supersaturations compared to laboratory activation fractions for 50 nm particles composed of ammonium sulfate (Fig. 4e, shown here for a supersaturation of 1%), a representative continental background aerosol. Overall, the case shown here is representative of typical aerosol measured during the early afternoon deployments, which had an average background concentration of 2500 cm^{-3} and an activation fraction of 0.4 at 1% supersaturation, while the AMF1 site observed higher concentrations and lower activation fractions. These site-to-site differences are likely due to differences in the size distributions and possibly in aerosol composition.

The TAMU miniMPL lidar collected a vertical profile of backscatter and depolarization by aerosols and cloud particles (Fig 4c). Surface aerosol, CCN, and INP measurements and sounding profiles are used as inputs to a vertical profile retrieval that uses these lidar backscatter measurements. Micropulse lidar and radiosonde data are used to calculate the aerosol backscatter coefficient profile, which was adjusted for aerosol hygroscopic growth. This corrected profile was then used to linearly scale surface measurements of aerosol, CCN, and INP concentrations. The preliminary retrieval of aerosol, CCN, and INP concentration profiles are shown in Figure 4g-h. A full description of these retrievals, their assumptions, and uncertainties will be described in another manuscript in preparation. These retrieved vertical profiles demonstrate the significant air mass heterogeneity between the sea- and bay-breeze air masses, with considerably lower aerosol and CCN concentrations over a shallower layer in the sea breeze air mass at the TAMU site. They also highlight the significant differences between surface aerosol, CCN, and INP concentrations and those near cloud base. The LCL is just above 1km, so at both sites, aerosol and CCN concentrations near cloud base are less than half of surface concentrations and INP concentrations near cloud base are 3-4 times smaller than the surface. This suggests that previous observational ACI studies only using surface-based aerosol concentrations may have significantly overestimated aerosols. These lidar-derived profile products represent a significant advance in our understanding of the vertical profiles of CCN and INP and can be used as input for real-case numerical simulations rather than some assumed profile based solely on surface aerosol number concentrations.

Accepted for publication in *Bulletin of the American Meteorological Society.* DOI 10.1175/BAMS-D-23-0218.1.

For the second, inland deployment on 8 August 2022, the TAMU team launched the radiosonde from Hempstead, TX at 2131 UTC. The sounding was launched earlier than the scheduled ARM site launch at 2200 UTC due to an approaching outflow boundary, which eventually arrived at Hempstead around 2208 UTC (Fig. 5b). This enabled the sampling of a continental air mass at Hempstead (TAMU site), while radiosondes from both ARM sites sampled a maritime air mass at 2200 UTC. As a result, the TAMU observations provide the only measurements of the undisturbed continental air mass for cells initiating along and ahead of the sea-breeze front at this time.

Considerable mesoscale heterogeneity in CAPE persisted during the second (late afternoon) deployment (Fig. 5a). The continental air mass at the inland TAMU site exhibited a deep and well-mixed planetary boundary layer (PBL), albeit with a lower relative humidity (RH) compared to the ARM sites (TAMU=44%, AMF1/ANC>60%). The well-mixed and moist PBL at the ANC site (not shown) significantly contributed to the MLCAPE value of 1719 J kg^{-1}, which was the largest among the three sites. The reduced MLCAPE at the other two sites (TAMU=1192 J kg^{-1}, and AMF1=1438 J kg^{-1}) was due to the low water vapor mixing ratio within the lowest 150-hPa layer, as well as smaller lapse rates throughout the mid to upper-troposphere. These MLCAPE values for the 3 sites fall very close to the median-observed MLCAPE (1170 J kg^{-1} at TAMU, 1415 J kg^{-1} at AMF1, and 1628 J kg^{-1} at ANC) for all TAMU TRACER late afternoon deployments.

As expected, the timeseries of ROAM-V continental aerosols (Fig. 5b) showed higher concentrations than the background concentrations for the maritime air mass. There is also evidence of an enhancement in aerosols as an outflow boundary (evident in the SWS temperature and humidity measurements) overtakes the site just after 2205 UTC. Again, the mesoscale heterogeneity in aerosols and CCN accompanying the different air masses is showcased in the AMF1 and TAMU size distributions (Fig. 5d), activated fractions (Fig. 5e), and retrieved profiles (Fig. 5g-h). The AMF1 site, which was overtaken by the bay breeze and sea breeze and was also likely under the influence of earlier convection outflow boundaries, showed much lower concentrations, smaller sizes, and lower activated fractions compared to TAMU's observations of the continental air mass likely influencing many of the cells shown in Fig 1b. The case shown here is representative of the TAMU late afternoon deployments with higher average concentrations, around 6000 cm^{-3}, and greater average CCN activation fractions, near 0.5, at 1% supersaturation when compared to the average maritime

Accepted for publication in *Bulletin of the American Meteorological Society.* DOI 10.1175/BAMS-D-23-0218.1.

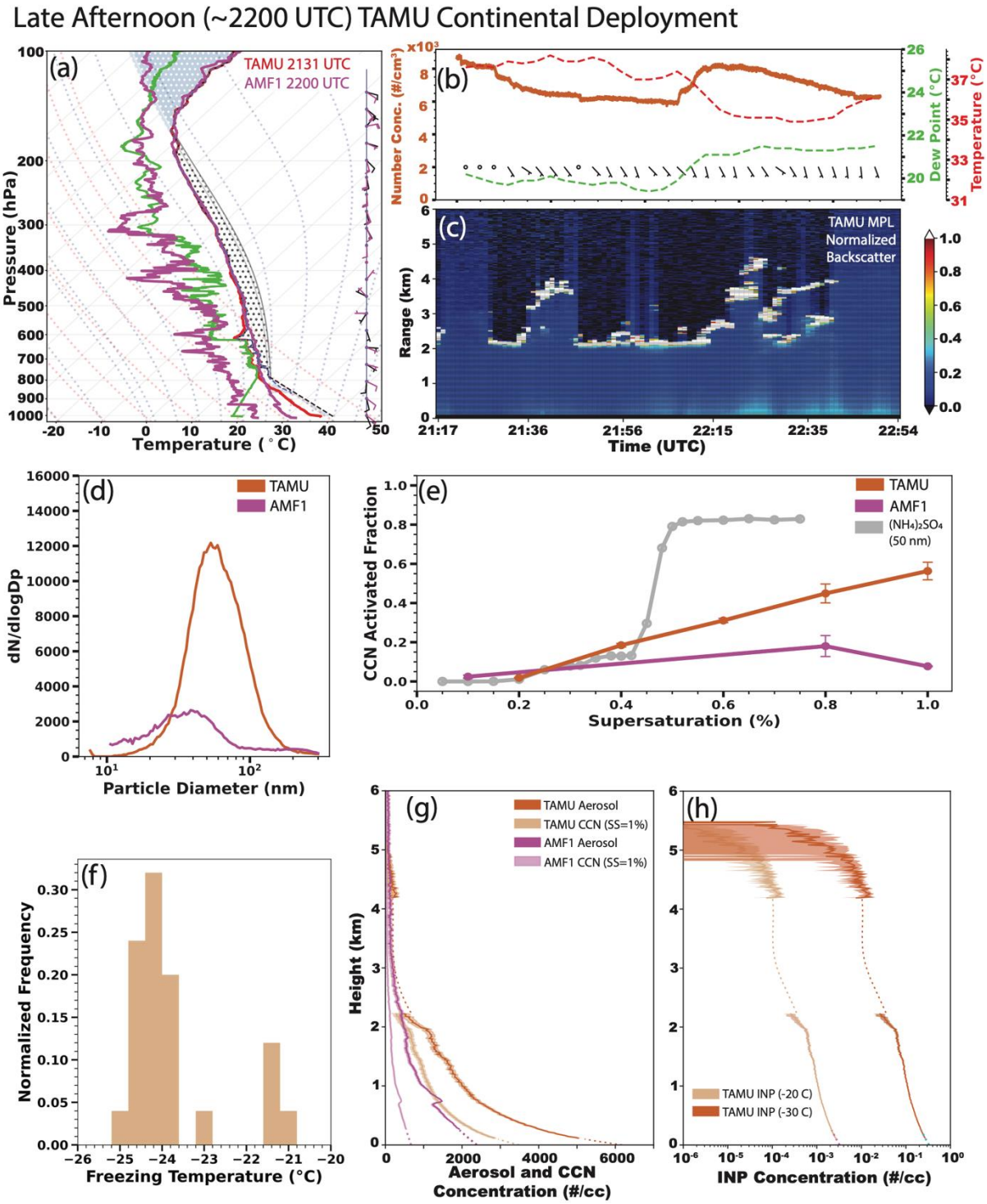

Figure 5 - a) 2200 UTC TAMU and AMF1 SkewT-logP comparison, b) CPC aerosol concentration and SWS temperature, dewpoint, and winds, c) miniMPL backscatter, d) TAMU and AMF1 SMPS aerosol size distributions, e) TAMU and AMF1 CCN activated fraction, f) INP freezing temperatures, g) TAMU and AMF1 retrieved profile of aerosol and CCN concentration, and h) retrieved TAMU INP concentration profile for afternoon continental deployment at City Park in Hempstead, TX on 8 August 2022. Shading on panels g) and h) represent the uncertainty range on the retrieved profiles due to lidar inversion process and hygroscopic growth corrections. Note that TAMU is shown in orange to represent the continental airmass sampling in the late afternoon with AMF1 maritime sampling still represented in magenta.

Accepted for publication in *Bulletin of the American Meteorological Society.* DOI 10.1175/BAMS-D-23-0218.1.

air mass. The retrieved vertical profiles also show important structural differences in the aerosol and CCN profiles, with the TAMU continental aerosol measurements showing a deep layer of increased aerosol and CCN concentrations extending nearly 2 km deeper than the AMF1 profiles. They again show significant differences in aerosols, CCN, and INP concentrations between the surface and cloud base that may be important for determining the impacts of ACI.

Planned analysis and science opportunities

The example cases shown here highlight some of the unique measurements collected by the TAMU TRACER team: collocated mobile meteorology and aerosol sampling, CCN and INP cloud forming properties, and retrievals of vertical profiles of CCN and INP concentrations in environments serving as the inflow region for convection. They also demonstrate the large spatial and temporal heterogeneity in the meteorological and aerosol environments across the Houston, TX region during the TRACER field campaign and the complementary dataset to the DOE fixed ARM site measurements collected by TAMU. From this case and others sampled during TRACER, it is clear that a single, fixed site cannot account for the heterogeneity of conditions experienced by convection in this region and that the environmental differences in the air mass serving as the inflow region for convection must be accounted for to have any hope of using observations to understand and disentangle the effects of aerosols and meteorology on deep convection.

Ultimately, we hope to use the TAMU measurements to quantify the ability of the complex aerosol populations in the Houston area to form CCN and INP (Thompson et al. 2024) and compare with ARM observations, use these observations to better constrain vertical CCN and INP profiles (Chen et al. 2024), and understand how meteorology and aerosol populations relate to observed changes in convection characteristics (Sharma et al. 2024). We also plan to use the measured meteorological environment and retrieved CCN and INP profiles as input for idealized numerical simulations to help disentangle meteorological effects from aerosol effects on deep convection updraft and precipitation characteristics. We envision a number of research questions that could be addressed by TAMU TRACER dataset including:

Accepted for publication in *Bulletin of the American Meteorological Society.* DOI 10.1175/BAMS-D-23-0218.1.

- What is the horizontal, vertical, and temporal variability of temperature, moisture, winds, and aerosols (specifically potential CCN and INP) in the Houston region, particularly relative to sea/bay-breeze fronts and outflow boundaries?
- How do the cloud forming properties of CCN and INP vary with the different mesoscale air masses observed during TRACER? How does cloud processing impact CCN and INP properties measured in convective outflow?
- How do updraft and precipitation characteristics vary with aerosols and meteorological environments across the sea/bay-breeze fronts?
- Do vertical distributions of CCN and INPs vary within the inflow layer of convection in different air masses in the Houston region? If so, might aerosol-cloud interactions influence deep convective updraft and precipitation characteristics? Do ACI results differ when assuming surface vs. cloud base aerosol concentrations?
- Does entrainment of aerosols above the storm inflow layer influence the thermodynamic properties, aerosol concentrations, and microphysical properties of deep convective updrafts?
- What are the separate influences of meteorological conditions and aerosols in determining updraft characteristics and precipitation processes in deep convection?

In addition to the aforementioned questions on air mass heterogeneity across the sea-breeze front and its influence on the properties of convection, the time series data in the examples shown here also highlight additional science opportunities for understanding the evolution of boundary layer thermodynamics and aerosol populations. During TAMU TRACER, we sampled the passage of the sea-breeze front, numerous outflow boundaries, anvil shading influences, and air mass recovery from prior convection. Thus, our data may be useful to future investigators in answering a host of science questions beyond those posed above. All TAMU TRACER data are freely available at the DOE ARM Data Discovery.

Acknowledgements

Accepted for publication in *Bulletin of the American Meteorological Society.* DOI 10.1175/BAMS-D-23-0218.1.

This project is funded by Department of Energy Atmospheric System Research (ASR) program grant DE-SC0021047 and supported by ARM field campaigns AFC07023, AFC07055. Some undergraduate participants were also supported by Texas A&M University College of Arts & Sciences (formerly Geosciences) High Impact Learning Experience grant. Special thanks to: Dr. Don Conlee and TAMU students C. Hood, P. Langford, S. Lewis, C. Perez, B. Tomerlin, J. Treviño, B. Musall, M. Mancilla, K. Nunez, T. Borgstedte, K. Griese, T. Peña, S. Alegrias, L. Mata-Rodriguez, R. Lane, B. Kropp, S. Gardner, J. Ribail, J. Hale, S. Butler, K. Lange, J. Lewis, A. Sebok, D. Leathe, S. Jorgensen, B. Smith, J. Spotts, and D. Topping for assisting with TAMU TRACER and broader DOE TRACER forecasting, nowcasting, deployments, and instrumentation. We also appreciate I.T. Holleman Elementary School and Buc-ees #18 in Waller, TX for allowing use of their facilities for several multi-hour deployments.

Data Availability Statement

TAMU TRACER data are available for download from the ARM Data Center through Data Discovery at https://doi.org/10.5439/1968819 (radiosonde), https://doi.org/10.5439/1972461 (MPL), https://doi.org/10.5439/1971998 (CPC), https://doi.org/10.5439/1972181 (SMPS), https://doi.org/10.5439/1972179 (CCN counter). ARM AMF1 data are available to download from the ARM Data Center through Data Discovery at https://doi.org/10.5439/1595321 (radiosonde), https://doi.org/10.5439/1320657 (MPL), https://doi.org/10.5439/1228061 (CPC), https://doi.org/10.5439/1476898 (SMPS), https://doi.org/10.5439/1323892 and https://doi.org/10.5439/1323896 (CCN counter). KHGX level-II data can be downloaded from the National Centers for Environmental Information (NCEI) NEXRAD data inventory (NOAA National Weather Service (NWS) Radar Operations Center 1991) at https://doi:10.7289/V5W9574V.

REFERENCES

Atkinson, D. B., P. Massoli, N. T. O'Neill, P. K. Quinn, S. D. Brooks, S. D., and B. Lefer, 2010: Comparison of in situ and columnar aerosol spectral measurements during TexAQS-GoMACCS 2006: testing parameterizations for estimating aerosol fine mode properties. *Atmos. Chem. Phys*., **10**, 51–61, doi:10.5194/acp-10-51-2010.

Accepted for publication in *Bulletin of the American Meteorological Society.* DOI 10.1175/BAMS-D-23-0218.1.

Carrio, G. G., W.R. Cotton, and W.Y.Y. Cheng, 2010: Urban growth and aerosol effects on convection over Houston Part I: The August 2000 case. *Atmos. Res*., **96**, 560–574, doi:10.1016/j.atmosres.2010.01.005, 2010.

Chen, B., S.A. Thompson, B.H. Matthews, M. Sharma, R. Li, C.J. Nowotarski, A.D. Rapp, and S.D. Brooks, 2024: Retrieving vertical profiles of aerosols and their cloud nucleating properties using a Micropulse lidar, *104th Annual Meeting*, Baltimore, MD, Amer. Meteor. Soc., 12.4, https://ams.confex.com/ams/104ANNUAL/meetingapp.cgi/Paper/433969.

Daum, P. H., L. I. Kleinman, S. R. Springston, L. J. Nunnermacker, Y. N. Lee, J. Weinstein-Lloyd, J. Zheng, and C. M. Berkowitz, 2004: Origin and properties of plumes of high ozone observed during the Texas 2000 Air Quality Study (TexAQS 2000). *J. Geophys. Res.*, **109**, D17306, https://doi.org/10.1029/2003JD004311.

Fan, J., and T. Yuan, J.M. Comstock, S. Ghan, A. Khain, L.R. Leung, Z. Li, V.J. Martins, M. Ovchinnikov, 2009: Dominant role by vertical wind shear in regulating aerosol effects on deep convective clouds. *J. Geophys. Res*., **114**, D22206, doi:10.1029/2009JD012352.

Fan, J., L. R. Leung, D. Rosenfeld, Q. Chen, Z. Li, J. Zhang, and H. Yan, 2013: Microphysical effects determine macrophysical response for aerosol impacts on deep convective clouds. *Proc. Natl. Acad. Sci. USA*, **110**, E4581–E4590, doi:10.1073/pnas.1316830110.

Fan, J., D. Rosenfeld, Y. Ding, L.R. Leung, & Z. Li, 2012: Potential aerosol indirect effects on atmospheric circulation and radiative forcing through deep convection. *Geophys. Res. Lett.*, **39**.

Fan, J., D. Rosenfeld, Y. Zhang, S.E. Giangrande, Z. Li, L.A.T. Machado, S.T. Martin, Y. Yang, J. Wang, P. Artaxo, H.M.J. Barbosa, R. Braga, J.M. Comstock, Z. Feng, W. Gao, H.B. Gomes, F. Mei, C. Poehlker, M. Poehlker, U. Poeschl, and R.A.F. de Souza, 2018: Substantial convection and precipitation enhancements by ultrafine aerosol particles. *Science*, **359**, 411–418.

Fan, J., R. Zhang, W.K. Tao, & K.I. Mohr, 2008: Effects of aerosol optical properties on deep convective clouds and radiative forcing. J. of Geophys. Res., **113**, D08209. doi:10.1029/2007JD009257.

Accepted for publication in *Bulletin of the American Meteorological Society.* DOI 10.1175/BAMS-D-23-0218.1.

Fridlind, A.M., M. van Lier-Walqui, S. Collis, S.E. Giangrande, R.C. Jackson, X. Li, T. Matsui, R. Orville, M.H. Picel, D. Rosenfeld, A. Ryzhkov, R. Weitz, and P. Zhang, 2019: Use of polarimetric radar measurements to constrain simulated convective cell evolution: A pilot study with Lagrangian tracking: *Atmospheric Measurement Techniques,* **12**(6), 2979-3000.

Ghan, S. J., and D.R. Collins, 2004: Use of in situ data to test a Raman lidar–based cloud condensation nuclei remote sensing method. *J. Atmos. and Oceanic Technol*., **21**, 387-394.

Ghan, S. J., T.A. Rissman, R. Elleman, R.A. Ferrare, D. Turner, C. Flynn, J. Wang, J. Ogren, J. Hudson, and H.H. Jonsson, 2006: Use of in situ cloud condensation nuclei, extinction, and aerosol size distribution measurements to test a method for retrieving cloud condensation nuclei profiles from surface measurements. *J. Geophys. Res. Atmos*., **111**, D05S10, doi:10.1029/2004JD005752.

Hu, J. X., D. Rosenfeld, A. Ryzhkov, D. Zrnic, E. Williams, P.F. Zhang, J.C. Snyder, R.Y. Zhang, and R. Weitz, 2019: Polarimetric Radar Convective Cell Tracking Reveals Large Sensitivity of Cloud Precipitation and Electrification Properties to CCN. *J. Geophys. Res.-Atmos.*, **124**, 12194–12205, doi:10.1029/2019jd030857.

IPCC, 2021: Climate Change 2021: The Physical Science Basis. Contribution of Working Group I to the Sixth Assessment Report of the Intergovernmental Panel on Climate Change. Cambridge University Press, 2391 pp., doi:10.1017/9781009157896.

Jensen, M.P., and Coauthors, 2019: Tracking Aerosol Convection Interactions ExpeRiment (TRACER) Science Plan. DOE/SC-ARM-19-017, 39pp, https://www.arm.gov/publications/programdocs/doe-sc-arm-19-017.pdf

Jin, M., J. M. Shepherd, and M. D. King, 2005: Urban aerosols and their variations with clouds and rainfall: A case study for New York and Houston. *J. Geophys. Res*., **110**, D10S20, doi:10.1029/2004JD005081.

Kanji, Z. A., Ladino, L. A., Wex, H., Boose, Y., Burkert-Kohn, M., Cziczo, D. J., & Krämer, M., 2017: Overview of ice nucleating particles. *Meteorol. Monographs*, **58**, 1.1-1.33.

Khain, A. P., 2009: Notes on state-of-the-art investigations of aerosol effects on precipitation: A critical review. *Environ. Res. Lett*., **4**, 015004, doi:10.1088/1748-9326/4/1/015004.

Accepted for publication in *Bulletin of the American Meteorological Society.* DOI 10.1175/BAMS-D-23-0218.1.

Khain, A. P., and M. Pinsky, 2018: *Physical Processes in Clouds and Cloud Modeling*. Cambridge University Press, 642 pp.

Khairoutdinov, M. F., and C.-E. Yang, 2013: Cloud-resolving modelling of aerosol indirect effects in idealised radiative convective equilibrium with interactive and fixed sea surface temperature. *Atmos. Chem. Phys*., **13**, 4133–4144, doi:10.5194/acp-13-4133-2013.

Koren, I., L. A Remer, O. Altaratz, J. V. Martins, and A. Davidi, 2010: Aerosol-induced changes of convective cloud anvils produce strong climate warming. *Atmos. Chem. Phys.* **10**, 5001–5010.

Lamer, K., P. Kollias, E. P. Luke, B. P. Treserras, M. Oue, and B. Dolan, 2023: Multisensor Agile Adaptive Sampling (MAAS): A methodology to collect radar observations of convective cell lifecycle. *J. Atmos. and Oceanic Tech.*, **40**, 1509-1522, doi:10.1175/JTECH-D-23-0043.1.

Lebo, Z. J., 2014: The sensitivity of a numerically simulated idealized squall line to the vertical distribution of aerosols. *J. Atmos. Sci.,* **71,** 4581-4596.

Lenhardt, E. D., L. Gao, J. Redemann, F. Xu, S.P. Burton, B. Cairns, I. Chang, R.A. Ferrare, C.A. Hostetler, and P.E. Saide, 2023: Use of lidar aerosol extinction and backscatter coefficients to estimate cloud condensation nuclei (CCN) concentrations in the southeast Atlantic. *Atmos. Measurement Tech*., **16**, 2037-2054.

Lin, L., Y. Xu, Z. Wang, C. Diao, W. Dong, and S.-P. Xie, 2018: Changes in extreme rainfall over India and China attributed to regional aerosol–cloud interaction during the late 20th century rapid industrialization. *Geophys. Res. Lett*., **45**, 7857–7865.

Marinescu, P. J., and Coauthors, 2021: Impacts of varying concentrations of cloud condensation nuclei on deep convective cloud updrafts—A multimodel assessment. *J. Atmos. Sci.*, **78**, 1147–1172, doi.org:10.1175/JAS-D-20-0200.1.

Marinou, E., M. Tesche, A. Nenes, A. Ansmann, J. Schrod, D. Mamali, A. Tsekeri, M. Pikridas, H. Baars, and R. Engelmann, 2019: Retrieval of ice-nucleating particle concentrations from lidar observations and comparison with UAV in situ measurements. *Atmos. Chem. Phys*., **19**, 11315-11342.

Accepted for publication in *Bulletin of the American Meteorological Society.* DOI 10.1175/BAMS-D-23-0218.1.

Orville, R. E., and Coauthors, 2001: Enhancement of cloud-to-ground lightning over Houston, Texas. *Geophys. Res. Lett*., **28**, 2597–2600, doi:10.1029/2001GL012990.

Parrish, D. D., D. T. Allen, T. S. Bates, M. Estes, F. C. Fehsenfeld, G. Feingold, R. Ferrare, R. M. Hardesty, J. F. Meagher, J. W. Nielsen-Gammon, R. B. Pierce, T. B. Ryerson, J. H. Seinfeld, and E. J. Williams, 2009: Overview of the second Texas Air Quality Study (TexAQS II) and the Gulf of Mexico atmospheric composition and climate study (GoMACCS). *J. Geophys. Res.*, **114**, D00F13, doi:10.1029/2009JD011842.

Peng, J., Z. Li, H. Zhang, J. Liu, and M. Cribb, 2016: Systematic changes in cloud radiative forcing with aerosol loading for deep clouds in the tropics. *J. Atmos. Sci*., **73**, 231–249, doi:10.1175/JAS-D-15-0080.1.

Ren, T., A. D. Rapp, J. Mecikalski, and J. Apke, 2019: Lightning and associated convection features in the presence of absorbing aerosols over northern Alabama. *J. Geophys. Res. Atmos.,* **124**, 13375-13396, doi: 10.1029/2019JD031544.

Ren, T., A. D. Rapp, S. Nasiri, J. Mecikalski, and J. Apke, 2018: Is awareness of the aerosol state useful in predicting enhanced lightning for lightning-producing storms over northern Alabama? *J. Appl. Meteor. Clim*., 57, 1663-1681.

Rosenfeld, D., U. Lohmann, G. B. Raga, C. D. O'Dowd, M. Kulmala, S. Fuzzi, A. Reissell, and M. O. Andreae, 2008: Flood or drought: How do aerosols affect precipitation? *Science*, **321**, 1309–1313, doi:10.1126/science.1160606.

Sharma, M., A.D. Rapp, C.J. Nowotarski, and S.D. Brooks, 2024: Observed variability in convective cell characteristics and near-storm environments across the sea and bay-breeze fronts in southeast Texas. In revision for *Mon. Wea. Rev.*

Teller, A., and Z. Levin, 2006: The effects of aerosols on precipitation and dimensions of subtropical clouds: A sensitivity study using a numerical cloud model. *Atmos. Chem. Phys*., **6**, 67–80, doi:10.5194/acp-6-67-2006

Tao, W.-K., J.-P. Chen, Z. Li, C. Wang, and C. Zhang, 2012: Impact of aerosols on convective clouds and precipitation. *Rev. of Geophys*., **50**, RG2001, https://doi.org/10.1029/2011RG000369.

Thompson, S.A., S.D. Brooks, A.D. Rapp, C.J. Nowotarski, B. Matthews, B. Chen, and R. Li, 2023: Characterization of cloud-forming properties for maritime and continental

Accepted for publication in *Bulletin of the American Meteorological Society.* DOI 10.1175/BAMS-D-23-0218.1.

aerosols across Houston during TRACER. *AGU 2023 Fall Meeting*, San Francisco, CA, Amer. Geophys. Union, A43D-05, https://agu.confex.com/agu/fm23/meetingapp.cgi/Paper/1252728.

van den Heever, S. C., G. Carrio, W. R. Cotton, P. J. DeMott, and A. J. Prenni, 2006: Impacts of nucleating aerosol on Florida convection: Part I. Mesoscale simulations. *J. Atmos. Sci*., **63**,1752–1775, doi:10.1175/JAS3713.1.

Wang, C., 2005: A model study of the response of tropical deep convection to the increase of CCN concentration: 1. Dynamics and microphysics. *J. Geophys. Res*., **110,** D21211, doi:10.1029/2004JD005720.

Williams, E., , D. Rosenfeld, N. Madden, J. Gerlach, N. Gears, L. Atkinson, N. Dunnemann, G. Frostrom, M. Antonio, B. Biazon, R. Camargo, H. Franca, A. Gomes, M. Lima, R. Machado, S. Manhaes, L. Nachtigall, H. Piva, W. Quintiliano, L. Machado, P. Artaxo, G. Roberts, N. Renno, R. Blakeslee, J. Bailey, D. Boccippio, A. Betts, D. Wolff, B. Roy, J. Halverson, T. Rickenbach, J. Fuentes, E. Avelino 2002: Contrasting convective regimes over the Amazon: Implications for cloud electrification. *J. Geophys. Res*., **107**, 8082, doi:10.1029/2001JD000380.

Wright, M.E., D.B. Atkinson, L. Ziemba, R. Griffin, N. Hiranuma, S. Brooks, B. Lefer, J. Flynn, R. Perna, B. Rappenglück, W. Luke, P. Kelley, 2010: Extensive aerosol optical properties and aerosol-mass related measurements during TRAMP/TexAQS 2006 – implications for PM compliance and planning. *Atmos. Environ*., **44** (33), 4035-4044.

Yan, H. R., Z. Q. Li, J. P. Huang, M. Cribb, and J. J. Liu, 2014: Long-term aerosol-mediated changes in cloud radiative forcing of deep clouds at the top and bottom of the atmosphere over the Southern Great Plains. *Atmos. Chem. Phys*., **14**, 7113–7124, doi:10.5194/acp-14-7113-2014.

Zhang, Y., J. Fan, Z. Li, and D. Rosenfeld, 2021: Impacts of cloud microphysics parameterizations on simulated aerosol–cloud interactions for deep convective clouds over Houston. *Atmos. Chem. Phys.*, **21**, 2363–2381, doi:10.5194/acp-21-2363-2021, 2021.

Accepted for publication in *Bulletin of the American Meteorological Society.* DOI 10.1175/BAMS-D-23-0218.1.